


Analysis of the $K^-p \rightarrow \gamma\Lambda$ reaction*

Yi Pan (潘一)^{1,2} Rong Li (李荣)^{1,2} Bo-Chao Liu (刘伯超)^{1,2†} 

¹MOE Key Laboratory for Nonequilibrium Synthesis and Modulation of Condensed Matter, School of Physics, Xi'an Jiaotong University, Xi'an 710049, China

²Institute of Theoretical Physics, Xi'an Jiaotong University, Xi'an 710049, China

Abstract: In this work, we study the $K^-p \rightarrow \gamma\Lambda$ reaction in an effective Lagrangian approach and isobar model. Compared to previous studies using a Regge-plus-resonance model, we consider the contributions of the t -channel (K and K^*) and u -channel (proton) exchanges explicitly as the background contribution. To restore the gauge invariance of the amplitude violated by introducing the phenomenological form factors, we employ two different methods from the literature. Then, we discuss the roles of possible resonance contributions in this reaction and present predictions of Λ polarization based on various models. We find that the contribution of the background terms plays an important role in the present reaction. Meanwhile, the $\Lambda(1520)$, $\Sigma(1660)$, and $\Sigma(1670)$ resonances may also contribute to this reaction. Due to the uncertainties of the present data and relatively small contributions of the hyperon resonances, we cannot identify the roles of various hyperon resonances in the present work. However, we show that the measurement of the spin polarization of the final Λ will be helpful to verify various models.

Keywords: hyperon resonance, Lambda polarization, gauge invariance

DOI: 10.1088/1674-1137/ada7ce **CSTR:** 32044.14.ChinesePhysicsC.49044106

I. INTRODUCTION

Studies of hadron production in electromagnetic and hadronic scattering processes are crucial for our knowledge of the hadron spectrum and understanding of the strong interaction in the low energy regime. Our present knowledge on the light baryon spectrum mainly comes from the analysis of old πN and $\bar{K}N$ scatterings and the more recent electron and photon induced reactions. In particular, due to the high quality of γN scattering data, in the last decade, there has been significant progress in studying the light baryon resonances [1]. Along with the significant progress in understanding of the photon induced reactions, it should also be interesting to further explore the crossing channels of these reactions. On the one hand, based on the models constrained by studies of the photon induced reactions, more reliable predictions for the crossing channels can be anticipated. On the other hand, studies of the crossing channels can offer further tests on the theoretical models employed in the photon induced reactions, which may help us to better understand the underlying dynamics of all the related reactions.

In the present work, we focus our interest on the

$K^-p \rightarrow \gamma\Lambda$ reaction, which is crossing-related to the $\gamma p \rightarrow K^+\Lambda$ reaction. For the latter reaction, there have been extensive studies both theoretically and experimentally. Due to isospin conservation in strong interactions, Δ resonances cannot couple to the $K\Lambda$ channel. Therefore, the $\gamma p \rightarrow K^+\Lambda$ reaction offers an ideal place to study the nucleon resonances with strong coupling with the $K\Lambda$ channel and to look for missing resonances. Before 2004, without high-quality experimental data, there were already many theoretical studies on this reaction [2–5]. Later, the high quality data published by the CLAS and LEPs Collaborations offered a very good basis for studying the properties of nucleon resonances and inspired further theoretical analysis of this reaction using different models, such as the isobar model [6–13], dynamical coupled-channel analysis [14–17], and Regge-plus-resonance (RPR) model [18, 19]. Along with the theoretical model adopted in this work, here, we focus on the works employing isobar models, which have been shown to be useful for analyzing the $\gamma p \rightarrow K^+\Lambda$ reaction. In the literature, although various isobar models can give quantitatively good descriptions of the data, they differ in describing the reaction mechanisms and model ingredients, such

Received 12 October 2024; Accepted 7 January 2025; Published online 8 January 2025

* Supported from the National Natural Science Foundation of China (U1832160) and the Natural Science Foundation of Shaanxi Province, China (2024JC-YBMS-010)

† E-mail: liubc@xjtu.edu.cn

©2025 Chinese Physical Society and the Institute of High Energy Physics of the Chinese Academy of Sciences and the Institute of Modern Physics of the Chinese Academy of Sciences and IOP Publishing Ltd. All rights, including for text and data mining, AI training, and similar technologies, are reserved.

as coupling constants, form factors, or the gauge invariance restoration (GIR) procedure. It is evident that some further studies are still necessary to verify various models and clarify the reaction mechanism.

To further explore and understand these models, it is useful to extend the models to study the crossing-related $K^-p \rightarrow \gamma\Lambda$ reaction. In fact, the idea that studying the crossing-related reactions may put further constraints on the model was realised long ago [7, 20]. However, previous theoretical studies on the $K^-p \rightarrow \gamma\Lambda$ reaction were conducted almost 30 years ago, and studies based on the models developed in recent years are still missing. In addition, some new data for the $K^-p \rightarrow \gamma\Lambda$ reaction were published in 2010 [21], which seems to have received little attention. Therefore, it is meaningful to analyze these data using models consistent with recent studies of the $\gamma p \rightarrow K^+\Lambda$ reaction, which constitutes one of the main purposes of this work. The other purpose of this work is to study the role of hyperon resonance in the present reaction while adopting different GIR methods. It should be noted that in the experimental analysis [21], the roles of hyperon resonances, such as $\Lambda(1520)$, $\Sigma(1660)$, and $\Sigma(1670)$, were discussed using the RPR model [18, 19]. Their studies showed that non-resonant contributions might play an important role in the present reaction. Because a different GIR method will lead to a different background contribution, it will also be interesting to explore and test the GIR methods in this reaction.

The remainder of this paper is organized as follows. In Sec. II, the theoretical model and ingredients for the reaction $K^-p \rightarrow \gamma\Lambda$ are presented. In Sec. III, we discuss the gauge invariance restoration methods employed in this work. In Sec. IV, the numerical results are presented with some discussions. Finally, this paper ends with a short summary in Sec. IV.

II. MODEL AND INGREDIENTS

In this section, we present the theoretical model and related ingredients employed in this work. In our model, we consider the s -channel hyperon and hyperon resonance exchanges, the t -channel K and K^* exchanges, the u -channel proton exchange, and a contact term. We neglect potential contributions from nucleon resonance exchanges in the u -channel due to the limited knowledge of the $N^*\Lambda K$ couplings for low-lying nucleon resonances. Moreover, their contributions are expected to be minor because the exchanged nucleon resonance is far off-shell. The Feynman diagrams for the $K^-(p_K) + p(p_p) \rightarrow \gamma(k) + \Lambda(p_\Lambda)$ reaction are shown in Fig. 1, with the symbols in parentheses denoting the four-momenta of the particles.

For s -channel resonance contributions, we consider $\Lambda(1520)(\frac{3}{2}^-)$, $\Sigma(1660)(\frac{1}{2}^+)$, and $\Sigma(1670)(\frac{3}{2}^-)$ in the intermediate states, as they lie in the energy region under

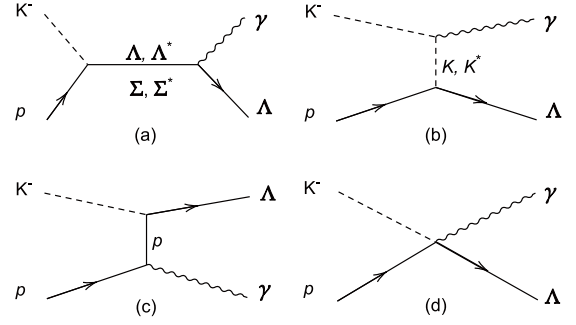


Fig. 1. Feynman diagrams for the $K^-p \rightarrow \gamma\Lambda$ reaction with Λ^* denoting $\Lambda(1520)$ and Σ^* denoting the $\Sigma(1660)$ or $\Sigma(1670)$.

study and may have significant coupling to the $\gamma\Lambda$ channel [22, 23]. It should be noted that, according to the PDG book [24], the couplings of $\Sigma(1660)$ and $\Sigma(1670)$ to the $\gamma\Lambda$ channel are still not well identified experimentally. To describe the couplings of the relevant vertices, the interaction Lagrangian densities are needed. The vertices involving the hyperon and hyperon resonances are considered as [25, 26]

$$\mathcal{L}_{\gamma\Lambda\Lambda} = \frac{e\kappa_\Lambda}{2M_\Lambda} \bar{\Lambda} \sigma^{\mu\nu} \partial_\nu A_\mu \Lambda, \quad (1)$$

$$\begin{aligned} \mathcal{L}_{\gamma\Lambda\Sigma} &= \frac{e\kappa_\Sigma}{2M_\Sigma} \bar{\Lambda} \sigma^{\mu\nu} \partial_\nu A_\mu \Sigma + \text{H.c.}, \\ \mathcal{L}_{R\Lambda\gamma}^{1/2\pm} &= e \frac{g_{R\Lambda\gamma}}{2M_\Lambda} \bar{R} \Gamma^{(\pm)} \sigma_{\mu\nu} (\partial^\nu A^\mu) \Lambda + \text{H.c.}, \end{aligned} \quad (2)$$

$$\begin{aligned} \mathcal{L}_{R\Lambda\gamma}^{3/2\pm} &= -ie \frac{g_{R\Lambda\gamma}^{(1)}}{2M_\Lambda} \bar{R}_\mu \gamma_\nu \Gamma^{(\pm)} F^{\mu\nu} \Lambda \\ &+ e \frac{g_{R\Lambda\gamma}^{(2)}}{(2M_\Lambda)^2} \bar{R}_\mu \Gamma^{(\pm)} F^{\mu\nu} \partial_\nu \Lambda + \text{H.c.}, \end{aligned} \quad (3)$$

$$\mathcal{L}_{\Lambda NK} = \frac{g_{\Lambda NK}}{2M_N} \bar{\Lambda} \gamma^\mu (\partial_\mu K) \gamma_5 N + \text{H.c.}, \quad (4)$$

$$\mathcal{L}_{\Sigma NK} = \frac{g_{\Sigma NK}}{2M_N} \bar{\Sigma} \gamma^\mu (\partial_\mu K) \gamma_5 N + \text{H.c.}, \quad (5)$$

$$\mathcal{L}_{RNK}^{1/2\pm} = -g_{RNK} \bar{N} \Gamma^{(\pm)} \left[\left(\frac{1}{M_R \pm M_N} \partial \right) K \right] R + \text{H.c.}, \quad (6)$$

$$\mathcal{L}_{RNK}^{3/2\pm} = \pm \frac{g_{RNK}}{M_K} \bar{N} \Gamma^{(\mp)} (\partial^\alpha K) R_\alpha + \text{H.c.}, \quad (7)$$

where R represents $\Lambda(1520)$, $\Sigma(1660)$, or $\Sigma(1670)$ resonance, and the superscripts of $\mathcal{L}_{R\Lambda\gamma}$ and $\mathcal{L}_{R\Lambda K}$ denote the J^P quantum numbers of the R resonance appearing in the Lagrangians. $\Gamma^{(+)}$ and $\Gamma^{(-)}$ are γ_5 and 1, respectively. In the Lagrangians, e is the electron charge, and κ_Λ and κ_Σ

are the anomalous magnetic moments of the corresponding hyperons, taking the values $\kappa_\Lambda = -0.613$ and $\kappa_{\Sigma^0} = 1.61$. The coupling constant $g_{\Lambda NK}$ is taken as -14 , which is determined by the flavor $SU(3)$ symmetry relation [27, 28]. The coupling constants g_{RNK} can be obtained by using the PDG values for the partial widths. Meanwhile, the couplings of the $R\Lambda\gamma$ vertices are relatively unknown. For their values, we shall discuss them in Sec. IV.

For t -channel meson exchange contributions, we consider the K and K^* exchanges in the intermediate state. The relevant interaction Lagrangian densities are [26, 29]

$$\mathcal{L}_{\gamma KK} = ie [K^+ (\partial_\mu K^-) - K^- (\partial_\mu K^+)] A^\mu, \quad (8)$$

$$\mathcal{L}_{\gamma KK^*} = e \frac{g_{\gamma KK^*}}{M_K} \epsilon^{\mu\nu\rho\sigma} (\partial_\mu A_\nu) (\partial_\rho K_\sigma^*) K, \quad (9)$$

$$\mathcal{L}_{\Lambda NK^*} = -g_{\Lambda NK^*} \bar{\Lambda} \left[\left(\gamma^\mu - \frac{\kappa_{\Lambda NK^*}}{2M_N} \sigma^{\mu\nu} \partial_\nu \right) K_\mu^* \right] N + \text{H.c.} \quad (10)$$

where K_μ^* is the K^* field, and $F^{\mu\nu} = \partial^\mu A^\nu - \partial^\nu A^\mu$ is the field-strength tensor. The value of the electromagnetic coupling $g_{\gamma KK^*} = 0.413$ is determined by the radiative decay width of $K^* \rightarrow \gamma + K$ given by the PDG book [24]. We take the value of $g_{\Lambda NK^*}$ from Ref. [27, 29].

For the u -channel diagram, we consider the proton exchange in the intermediate state. To calculate the amplitude, we still need the Lagrangian for the γNN vertex, which is taken as

$$\mathcal{L}_{\gamma NN} = -e\bar{N} \left[\left(\gamma^\mu - \frac{\kappa_N}{2M_N} \sigma^{\mu\nu} \partial_\nu \right) A_\mu \right] N \quad (11)$$

with $\kappa_p = 1.793$ for the proton [24].

Finally, a contact interaction is also considered in this work, which is necessary for restoring gauge invariance of the amplitude. The corresponding interaction Lagrangian density is taken as

$$\mathcal{L}_{\gamma\Lambda NK} = ie \frac{g_{\Lambda NK}}{2M_N} \bar{\Lambda} \gamma^\mu A^\mu K \gamma_5 N + \text{H.c.} \quad (12)$$

The propagators of the intermediate states with spin J are denoted as S_J and taken as

$$S_0(q) = \frac{i}{q^2 - m^2}, \quad (13)$$

$$S_1^{\mu\nu}(q) = -\frac{i(g_{\mu\nu} - q_\mu q_\nu / m^2)}{q^2 - m^2}, \quad (14)$$

$$S_{\frac{1}{2}}(q) = \frac{i(\not{q} + m)}{q^2 - m^2 + im\Gamma}, \quad (15)$$

$$S_{\frac{3}{2}}^{\mu\nu}(q) = \frac{i(\not{q} + m)}{q^2 - m^2 + im\Gamma} \left[-g^{\mu\nu} + \frac{1}{3}\gamma^\mu \gamma^\nu + \frac{1}{3m}(\gamma^\mu q^\nu - \gamma^\nu q^\mu) + \frac{2}{3m^2}q^\mu q^\nu \right], \quad (16)$$

where q and m are the four-momenta and mass of the intermediate state, respectively.

In practice, to consider the internal structure of hadrons and off-shell effects, phenomenological form factors are usually introduced in the amplitude. For baryon and baryon resonance exchanges, we use the following form factor [29, 30]:

$$F(q^2) = \left(\frac{\Lambda_B^4}{\Lambda_B^4 + (q^2 - M^2)^2} \right)^2, \quad (17)$$

where q and M are the four-momenta and mass of the intermediate particle, respectively, and Λ_B is the cutoff parameter. For meson exchanges, we use [29, 30]

$$f(q^2) = \left(\frac{\Lambda_M^2 - M^2}{\Lambda_M^2 - q^2} \right)^2. \quad (18)$$

The general amplitude of the $K^-p \rightarrow \gamma\Lambda$ reaction can be written as

$$M = \bar{u}_\Lambda \mathcal{M}^\mu \epsilon_\mu^* u_N, \quad (19)$$

where u_N and \bar{u}_Λ denote the Dirac spinors for the target nucleon and recoiled Λ , respectively, and ϵ_μ^* denotes the polarization vector of the outgoing photon. With the ingredients given above, it is straightforward to obtain the individual scattering amplitudes:

$$\mathcal{M}_{\frac{3}{2}^-,1}^\mu = \frac{e g_{R\Lambda\gamma} g_{RNK}^{(1)}}{2M_\Lambda M_K} (k_\nu \gamma^\mu S_{\frac{3}{2}}^{\nu\rho} - k S_{\frac{3}{2}}^{\mu\rho}) p_\rho^K \gamma_5 F_R, \quad (20)$$

$$\mathcal{M}_{\frac{3}{2}^-,2}^\mu = \frac{e g_{R\Lambda\gamma}^{(2)} g_{RNK}}{(2M_\Lambda)^2 M_K} (k_\nu p_\Lambda^\mu S_{\frac{3}{2}}^{\nu\rho} - k \cdot p_\Lambda S_{\frac{3}{2}}^{\mu\rho}) p_\rho^K \gamma_5 F_R,$$

$$\mathcal{M}_{\frac{1}{2}^+}^\mu = -\frac{e g_{R\Lambda\gamma} g_{RNK}}{2m_\Lambda M_R + M_N} k_\nu \sigma^{\mu\nu} S_{\frac{1}{2}} \not{p}_K \gamma_5 F_R, \quad (21)$$

$$\mathcal{M}_N^\mu = -i \frac{e g_{\Lambda NK}}{2M_N} \not{p}_K \gamma_5 S_{\frac{1}{2}} (\gamma^\mu - \frac{i\kappa_N}{2M_N} \sigma^{\mu\sigma} k_\sigma) F_p, \quad (22)$$

$$\mathcal{M}_K^\mu = -\frac{ie g_{\Lambda NK}}{M_N} p_K^\mu S_0 (\not{\epsilon} - \not{p}_K) \gamma_5 f_K, \quad (23)$$

$$\begin{aligned} \mathcal{M}_{K^*}^\mu &= -\frac{e g_{\gamma K K^*} g_{\Lambda N K^*}}{M_K} \epsilon^{\mu\nu\rho\sigma} k_\nu (k - p_K)_\rho S_{\sigma\lambda}^1 (\gamma^\lambda \\ &\quad - \frac{i k_{K^*}}{2M_N} \sigma^{\lambda\delta} (k - p_K)_\delta) f_{K^*}, \end{aligned} \quad (24)$$

$$\mathcal{M}_\Lambda^\mu = -\frac{e g_{\Lambda N K K_\Lambda}}{4M_N M_\Lambda} \sigma^{\mu\nu} k_\nu S_{\frac{1}{2}} \not{p}_K \gamma_5 F_\Lambda, \quad (25)$$

$$\mathcal{M}_\Sigma^\mu = -\frac{e g_{\Sigma N K K_\Sigma}}{4M_N M_\Sigma} \sigma^{\mu\nu} k_\nu S_{\frac{1}{2}} \not{p}_K \gamma_5 F_\Sigma, \quad (26)$$

$$\mathcal{M}_c^\mu = -i \frac{e g_{\Lambda NK}}{2M_N} \gamma^\mu \gamma_5 f_c. \quad (27)$$

The unpolarized differential cross-section for the reaction in the center-of-mass (c.m.) frame is given by

$$\frac{d\sigma}{d\Omega} = \frac{M_p M_\Lambda}{32\pi^2 s} \frac{|\vec{k}|}{|\vec{p}_K|} \sum_{\lambda, s_p, s_\Lambda} |\mathcal{M}_{fi}|^2, \quad (28)$$

where \mathcal{M}_{fi} is the total transition amplitude from initial to final state, $|\vec{k}|$ and $|\vec{p}_K|$ are the magnitudes of the three-momenta of the photon and K^- meson in the c.m. frame, respectively. The differential solid angle $d\Omega = d\cos\theta_\gamma d\phi$ corresponds to the direction of the outgoing photon, with θ_γ being the angle between the momenta of the photon and K^- meson in the c.m. frame. The sum runs over the helicity of the photon λ and the spin projections of the proton s_p and Λ particle s_Λ . Here, $s = (p_K + p_p)^2$ is the square of the total energy in the c.m. frame, where p_K and p_p are the four-momenta of the K^- meson and proton, respectively.

Furthermore, the spin polarization of the Λ particle can be calculated as

$$P_\Lambda = \frac{d\sigma_\uparrow - d\sigma_\downarrow}{d\sigma_\uparrow + d\sigma_\downarrow}, \quad (29)$$

where $d\sigma_\uparrow$ and $d\sigma_\downarrow$ are the differential cross-sections for the Λ particle with spin projections $+1/2$ and $-1/2$, respectively. The polarization axis is defined along the direction of $\vec{p}_K \times \vec{k}$ in the c.m. frame.

III. GAUGE INVARIANCE

As shown in the last section, the amplitudes corresponding to the Feynman diagrams shown in Fig. 1 can be drawn in a standard way. Meanwhile, due to the coupling of the electromagnetic field with the matter field, the full amplitude of this reaction should be invariant under

gauge transformations. It is well known that the introduction of form factors in the amplitude violates the gauge invariance of the amplitude of the Born terms, and it is desired to restore the gauge invariance through some phenomenological methods. In the literature, there are various methods to restore gauge invariance of the full amplitude for meson photoproduction processes [31–35]. In principle, such methods can also be applied to the crossing-related reaction $K^- p \rightarrow \gamma \Lambda$, which may offer a further test of the methods developed in studying the meson photoproduction processes and help understand the relevant reaction mechanisms better. In this work, we shall consider two different methods of restoring gauge invariance.

Here, we present the main ingredients and formulae of two GIR methods in the literature: Method A adopted in Ref. [32] and Method B adopted in Refs. [33–35]. For more details of the two methods, interested readers can refer to the corresponding references.

The Born amplitudes concerning the violation of gauge invariance can be written as

$$\mathcal{M}_B^\mu = \mathcal{M}_p^\mu + \mathcal{M}_K^\mu + \mathcal{M}_c^\mu. \quad (30)$$

Hence, the four-divergence of \mathcal{M}_B^μ is

$$k_\mu \mathcal{M}_B^\mu = \frac{ie g_{\Lambda NK}}{2M_N} [(\not{k} - \not{p}_K) f_K + \not{p}_K F_p - \not{k} f_c] \gamma_5, \quad (31)$$

where f_c is the form factor adopted for the contact term. Obviously, when considering form factors, gauge invariance is violated.

Method A: Following Davidson and Workman's prescription in Ref. [32], the form factor of the contact term is taken as

$$f_c = F_p + f_K - F_p f_K. \quad (32)$$

Then, the amplitude for the contact term is

$$\mathcal{M}_c^\mu = -ie \frac{g_{\Lambda NK}}{2M_N} \gamma^\mu \gamma_5 (F_p + f_K - F_p f_K) \quad (33)$$

To fulfill the gauge invariance condition $k_\mu \mathcal{M}^\mu = 0$, an additional term is added in the full amplitude, given by

$$\begin{aligned} \mathcal{M}_{\text{add}}^\mu &= -\frac{ie g_{\Lambda NK}}{2M_N} [(\not{k} - \not{p}_K) \frac{(2p_K - k)^\mu}{t - M_K^2} (F_p - F_p f_K) \\ &\quad + \not{p}_K \frac{(2p_p - k)^\mu}{u - M_N^2} (f_K - F_p f_K)] \gamma_5. \end{aligned} \quad (34)$$

By including this additional term, the resulting amplitude for the Born terms then satisfy the gauge invariance condition.

Method B: In this method, gauge invariance is guar-

anted by requiring that the full amplitude satisfies the generalized Ward-Takahashi identity (gWTI) [36, 37]. Following the logic of Ref. [33–35], the form factor of the contact term should be the same as the K exchange amplitude, *i.e.*, $f_C = f_K$. By introducing an auxiliary current, the additional term that needs to be added to the amplitude to restore the gauge invariance is written as

$$\mathcal{M}_{\text{add}}^\mu = \mathbf{G}(p_K)C^\mu \quad (35)$$

where $\mathbf{G}(p_K) = -\frac{ig_{\Lambda NK}}{2M_N}\not{p}_K$ describes the coupling structure of the ΛNK vertex, and C^μ is the auxiliary current. The auxiliary current C^μ is taken as

$$C^\mu = -e_K \frac{f_K - \hat{F}}{t - p_K^2} (2p_K - k)^\mu - e_p \frac{F_p - \hat{F}}{u - p_p^2} (2p_p - k)^\mu \quad (36)$$

with $\hat{F} = 1 - \hat{h}(1 - F_p)(1 - f_K)$. Here, in principle, \hat{h} is an arbitrary function of Mandelstam invariants going to unity in the high-energy limit, which is usually set to be unity for simplicity. In the present work, we also take $\hat{h} = 1$. Thus, we have $\hat{F} = F_p + f_K - F_p f_K$, which equals f_C in Method A. Therefore, we now have

$$\mathcal{M}_C^\mu = -ie \frac{g_{\Lambda NK}}{2M_N} \gamma^\mu \gamma_5 f_K \quad (37)$$

$$\begin{aligned} \mathcal{M}_{\text{add}}^\mu = & -\frac{ie g_{\Lambda NK}}{2M_N} \left[-\not{p}_K \frac{(2p_K - k)^\mu}{t - M_K^2} (F_p - F_p f_K) \right. \\ & \left. + \not{p}_K \frac{(2p_p - k)^\mu}{u - M_N^2} (f_K - F_p f_K) \right] \gamma_5. \end{aligned} \quad (38)$$

One can check that in this way that the four-divergence of $\mathcal{M}_B^\mu + \mathcal{M}_{\text{add}}^\mu$ satisfies the gWTI, which means that gauge invariance is restored.

Here, it is interesting to compare the resulting amplitude for the two methods. By comparing Eqs. (33) and (34) with Eqs. (37) and (38), it can be seen that both the contact term and additional term are different in the two methods. In Method A, the contact term is affected by the form factors F_p and f_K , while it only depends on f_K for Method B. For this reason, one can expect the contact term in Method A to be more closely related to the u -channel proton exchange contribution. For the additional term $\mathcal{M}_{\text{add}}^\mu$, the difference comes from the term proportional to \not{k} in Method A, which is absent in Method B. By inspecting the amplitudes obtained by the two methods, one can find that the difference is proportional to $F_p(1 - f_K)$. Therefore, it can be expected that the discrepancy between the two methods can be amplified with a large value of F_p and suppressed by a small value of F_p .

IV. RESULTS AND DISCUSSION

In this section, we present the numerical results and discussion. The experimental data for the $K^-p \rightarrow \gamma\Lambda$ reaction are taken from Ref. [21], where the angular distributions of the final photon at eight K^- momenta between 514 and 750 MeV were reported. The new data offer a chance to analyze the role of hyperon resonances in this energy region. Compared to the role of the nucleon resonances in the crossing-related $\gamma p \rightarrow K^+\Lambda$ reaction, in the present reaction, the s -channel contributions come from the excitation of the hyperon resonances in the intermediate states. In fact, the s - and u -channel contributions are rather different in these two reactions. Meanwhile, for the t -channel contribution and contact term, these two reactions are closely related, as they share the same interaction vertices and the physical regions of the t -channel contributions overlap. Furthermore, as illustrated in Sec. III, the t -channel K exchange and contact term contributions are also essential in the GIR procedure. Therefore, the study of the present reaction is helpful for studying the model dependence of the background contribution and the method for restoring gauge invariance.

It is well known that without introducing form factors, the Born terms alone will lead to a substantial overestimation of the total cross-sections of the $\gamma p \rightarrow K\Lambda$ reaction [4]. Thus, it is worth noting that we also find similar results for the $K^-p \rightarrow \gamma\Lambda$ reaction. Therefore, it is necessary to introduce form factors to suppress the contributions from the Born terms. Here, we adopt the form factor shown in Eqs. (17) and (18) for the Born terms and set the cutoff parameters Λ_M and Λ_B as free parameters, which are fitted to the experimental data. To avoid these parameters taking some unphysical values, we only allow these parameters to vary in a range of 0.5 to 2 GeV in the fittings. For the background contributions, the coupling constants are well known from the literature, so we just take the values from the literature and list them in Table 1. To reduce the number of parameters, we set the cutoff parameter for baryon resonances as 1.3 GeV, which is consistent with the values adopted in Ref. [39].

As the first step, we shall only consider the background contribution, as it was found that the background contribution alone in the RPR model could already give a reasonable description of data except for an underestimation of the data at forward angles [21]. As mentioned above, here, only the cutoff parameters in the form

Table 1. Values of coupling constants adopted in this work.

Parameter	Value	Parameter	Value
$g_{\Lambda NK}$	-14 [27, 28]	κ_p	1.793 [24]
$g_{\Lambda NK^*}$	-6.210 [27, 29]	κ_{K^*}	2.76 [29]
$g_{\gamma KK^*}$	0.413 [38]	κ_Λ	-0.613 [24]
$g_{\Sigma NK}$	2.69 [26, 27]	κ_Σ	1.61 [24]

factors, *i.e.*, Λ_M and Λ_B , will be treated as free parameters. By considering the two GIR methods discussed in the last section, the best fitting results for these two parameters are $\Lambda_M = 1.57$ GeV and $\Lambda_B = 0.5$ GeV for Method A and $\Lambda_M = 1.58$ GeV and $\Lambda_B = 0.5$ GeV for Method B. Here, we should mention that the value of $\Lambda_B = 0.5$ GeV is at the lower limit allowed in the fitting, which means that, in this case, the experimental data require a large suppression of the proton exchange contribution. Furthermore, we find that the background contributions in the two GIR methods are very similar. This is because the fitted value of Λ_B is small, which induces a small value of F_p and then a similar background contribution in the two methods, as discussed in the Sec. III. Therefore, we only plot the results using Method A (dashed line) in Fig. 2. As can be seen, using the fitted parameters, the background contribution indeed can give a relatively good description of the data ($\chi^2/dof = 1.12$). Compared to the RPR model [21], we get a slightly better description of the data at forward angles. This result indicates that background contribution may play an important role in this reaction. Meanwhile, it is expected that, in the *s*-channel, some hyperon resonances, *e.g.*, $\Lambda(1520)$, $\Sigma(1660)$, or $\Sigma(1670)$, may also contribute to the present reaction. However, at present, our knowledge on the properties of

hyperon resonances is rather limited. For the $\Lambda(1520)$, its couplings with $\gamma\Lambda$ and $\bar{K}N$ are relatively well studied. Meanwhile, the electromagnetic couplings of other hyperon resonances are still not known. Thus, as a next step, we shall only include the contribution from the $\Lambda(1520)$ exchange (Model I). Then, we will also discuss the possible contributions from $\Sigma(1660)$ (Model II) or $\Sigma(1670)$ (Model III) in the present reaction.

In this part, we shall consider both the background and $\Lambda(1520)$ contributions in this reaction. It should be noted that $\Lambda(1520)$ lies below the energies of the experimental data under study. Because current experimental data still have large uncertainties, it is not possible to constrain all the parameters of the $\Lambda(1520)$ amplitude simultaneously. Thus, we choose to fix the coupling constants of the $\Lambda(1520)\bar{K}N$ and $\Lambda(1520)\Lambda\gamma$ vertices using the PDG values of the corresponding partial decay widths. Note that for the $\Lambda(1520)\Lambda\gamma$ vertex, there are two independent Lagrangians, for which their relative magnitudes are still not well studied. To reduce the number of parameters, we only consider one of the two $\Lambda(1520)\Lambda\gamma$ couplings in the fitting. It turns out that the $\mathcal{L}^{(1)}$ coupling gives a better description of the data. Thus, in the following discussions, we shall concentrate on the results using the $\mathcal{L}^{(1)}$ coupling while taking $g_{\Lambda(1520)\bar{K}N} = 10.731$ and $g_{\Lambda(1520)\Lambda\gamma}^{(1)} = 1.356$,

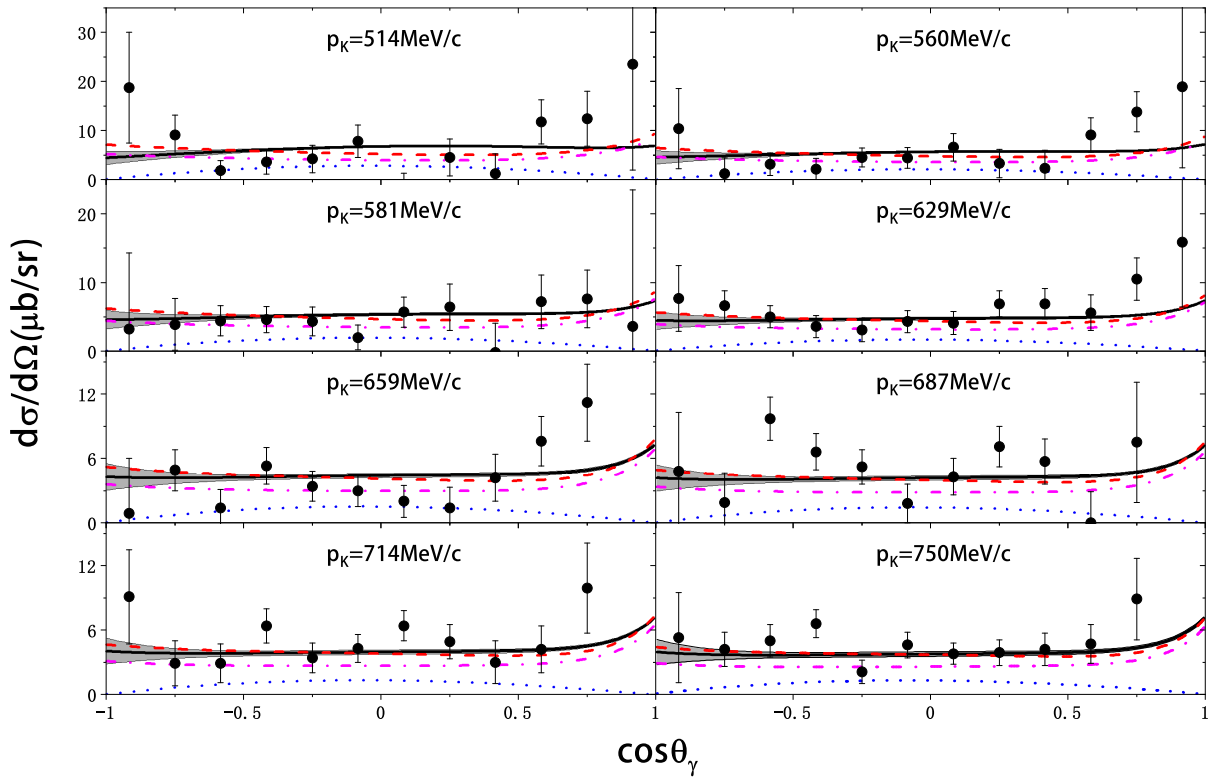


Fig. 2. (color online) Differential cross-sections for the $K^-p \rightarrow \gamma\Lambda$ reaction as a function of $\cos\theta_\gamma$, while only considering the background and $\Lambda(1520)$ contributions using Method A. The dashed line corresponds to the fitting results with only the background terms considered. The solid, dotted, and dot-dashed lines show the full, $\Lambda(1520)$, and background contributions in Model I, where the bands correspond to 1σ error regions of the fitting results.

Table 2. Fitted parameters considering both $\Lambda(1520)$ and $\Sigma(1660)$ (Model II).

Parameter	Method A	Method B
Λ_M	1.160 ± 0.124	1.247 ± 0.134
Λ_B	0.752 ± 0.088	0.931 ± 0.262
$\phi_{\Lambda(1520)}$	-1.520 ± 1.128	-1.635 ± 1.345
$g_{\Sigma(1660)\bar{K}N}g_{\Sigma(1660)\Lambda\gamma}$	-5.825 ± 1.170	6.241 ± 2.085
$\phi_{\Sigma(1660)}$	-0.401 ± 0.278	2.569 ± 0.538

which are determined using the PDG central values for the corresponding partial widths. In this way, the magnitude of the $\Lambda(1520)$ exchange contribution is fixed, and the only free parameter introduced for the $\Lambda(1520)$ amplitude is the relative phase, *i.e.*, $\phi_{\Lambda(1520)}$, between the $\Lambda(1520)$ amplitude and Born terms. By fitting the experimental data, the best results for the parameters in Model I are $\Lambda_M = 1.37 \pm 0.04$ GeV, $\Lambda_B = 0.5 \pm 0.16$ GeV, and $\phi_{\Lambda(1520)} = -1.55 \pm 0.53$ with $\chi^2/dof = 1.14$ for Method A and $\Lambda_M = 1.37 \pm 0.03$ GeV, $\Lambda_B = 0.59 \pm 0.15$ GeV, and $\phi_{\Lambda(1520)} = -1.47 \pm 0.52$ with $\chi^2/dof = 1.13$ for Method B. With these fitted parameters, we plot the angular distributions and make a comparison with the experimental data in Fig. 2. It seems that the inclusion of the $\Lambda(1520)$ contribution does not improve the fitting results. However,

because the magnitude of the $\Lambda(1520)$ contribution is fixed, the results also show that the PDG values for the $\Lambda(1520)\bar{K}N$ and $\Lambda(1520)\Lambda\gamma$ couplings are compatible with the current $K^-p \rightarrow \gamma\Lambda$ data. Due to the small value of Λ_B , it should not be surprising that the background contributions using the two GIR methods are similar here. Furthermore, we also find that the interference effects between the $\Lambda(1520)$ and background terms are small.

In the next step, we further include the contributions from the $\Sigma(1660)$ or $\Sigma(1670)$ resonances. We can deduce the couplings with the $\bar{K}N$ channel using the PDG value for the corresponding partial decay width. However, because their couplings to the $\Lambda\gamma$ channel are still unknown, and it is the product of $g_{\Sigma^*\bar{K}N}$ and $g_{\Sigma^*\Lambda\gamma}$ that appears in the amplitude, here, we treat their product, *i.e.*, $g_{\Sigma^*\bar{K}N}g_{\Sigma^*\Lambda\gamma}$, as a free parameter. Besides the coupling constants, we also introduce a phase factor for their amplitudes. In this way, by further considering $\Sigma(1660)$ (Model II) or $\Sigma(1670)$ (Model III), we have two more parameters ($g_{\Sigma^*\Lambda\gamma}g_{\Sigma^*\bar{K}N}$ and ϕ_{Σ^*}), and now the number of free parameters is 5. The best fitting results for the parameters of Model II are presented in Table 2. By further including $\Sigma(1660)$'s contribution, χ^2/dof can be reduced to 0.97 with Method A and 0.96 with Method B. By inspecting the fitted value of Λ_B , one may expect the discrepancies between the two GIR methods to be enhanced in this

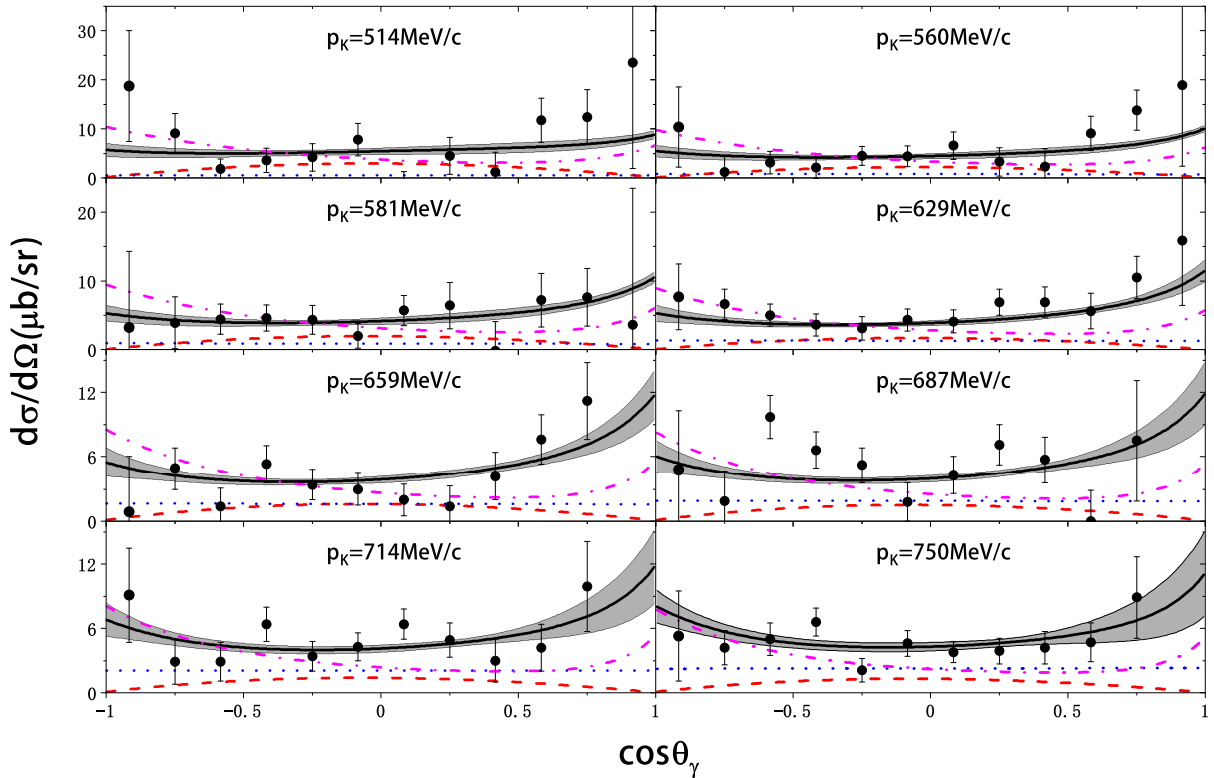


Fig. 3. (color online) Differential cross-sections for the $K^-p \rightarrow \gamma\Lambda$ reaction as a function of $\cos\theta_\gamma$ based on Model II. The solid, dashed, dotted, and dot-dashed lines show the results of the full amplitude, $\Lambda(1520)$, $\Sigma(1660)$, and background terms, respectively. The bands correspond to 1σ error regions of the fitting results.

case. We indeed find that there are some differences appearing in the background contribution at most backward angles using the two GIR methods. These discrepancies are also reflected in the different fitted parameters of $\Sigma(1660)$ using the two GIR methods, although they are consistent within the large uncertainties caused by the large errors of the experimental data at the forward and backward angles. Meanwhile, it should be noted that despite the differences in the background contributions, the full results for the angular distribution are still similar, because the differences in background contributions are compensated by a different $\Sigma(1660)$ contribution in the two GIR methods. Therefore, in Fig. 3, we only show the results of Model II using Method B.

The fitting results for the parameters of Model III are presented in Table 3. Including the contribution of $\Sigma(1670)$, χ^2/dof is reduced to 1.03 with Method A and 1.02 with Method B. Compared to the results of Model II, this shows that, using the current data, we cannot distinguish these two models well. Furthermore, due to the small value of Λ_B , we also find that the results using the two GIR methods are similar, as also reflected in the similarity of the fitted parameters. The results of Model III for the angular distribution using Method B are presented in Fig. 4. By comparing the results in Figs. 3 and 4, it is notable that there are prominent differences between the

Table 3. Fitted parameters considering both $\Lambda(1520)$ and $\Sigma(1670)$ (Model III).

Parameters	Method A	Method B
Λ_M	1.187 ± 0.084	1.186 ± 0.074
Λ_B	0.500 ± 0.187	0.602 ± 0.127
$\phi_{\Lambda(1520)}$	-0.959 ± 0.474	-0.942 ± 0.464
$g_{\Sigma(1670)\bar{K}N} g_{\Sigma(1670)\Lambda\gamma}$	6.161 ± 1.537	6.163 ± 1.512
$\phi_{\Sigma(1660)}$	3.939 ± 0.549	3.931 ± 0.547

background contributions in these two models, especially at backward angles. The difference mainly comes from the u -channel proton exchange and contact term contributions due to the different values obtained for Λ_B . In Fig. 5, we study the individual contributions to the total cross-sections using the two models. It can be seen that in both models, the background terms give important contributions. At the same time, $\Lambda(1520)$ may contribute significantly at the near-threshold region, and $\Sigma(1660)$ or $\Sigma(1670)$ may contribute at higher energies. In particular, considering the $\Sigma(1660)$ or $\Sigma(1670)$ contributions, the fitted background contribution changes significantly. In fact, in Model II, the background contribution is roughly a factor of 1.6 larger than that in Model III. This result shows that a reliable determination of the background contribution is

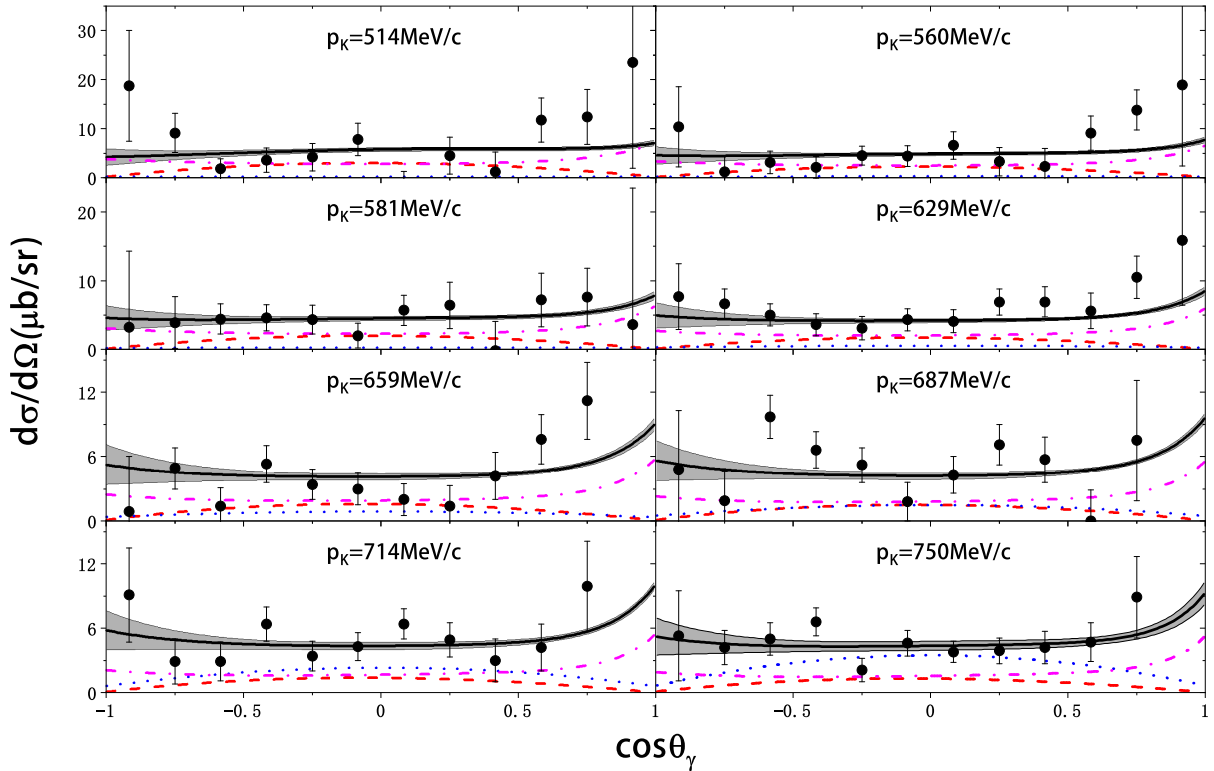


Fig. 4. (color online) Differential cross-sections for the $K^-p \rightarrow \gamma\Lambda$ reaction as a function of $\cos\theta_\gamma$, based on Model III. The solid, dashed, dotted, and dot-dashed lines show the results of the full amplitude, $\Lambda(1520)$, $\Sigma(1670)$ and background terms, respectively. The bands correspond to 1σ error regions of the fitting results.

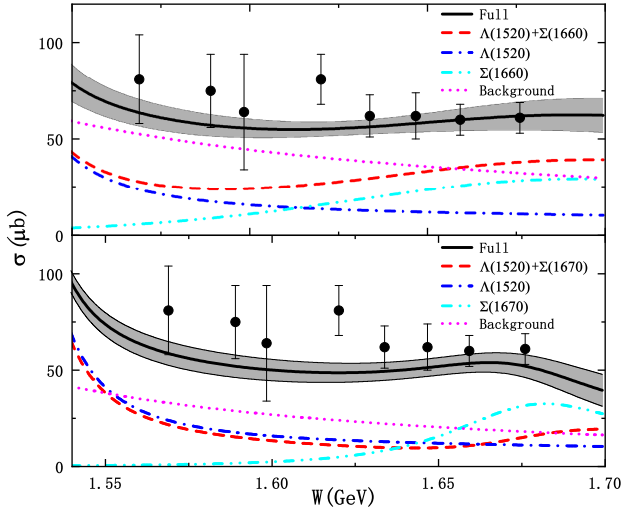


Fig. 5. (color online) Total cross-sections for the $K^- + p \rightarrow \gamma + \Lambda$ reaction using Model II (Top) and Model III (Bottom). The bands correspond to 1σ error regions of the fitting results.

crucial for investigating the role of s -channel resonances in this reaction.

It is also important to investigate the impact of uncertainties in the coupling constants listed in Table 1 on our fitting results. For the coupling constants $g_{\Lambda NK^*}$ and $g_{\Sigma NK}$, we find that their variations have a minimal impact on our results. This can be attributed to the relatively minor contributions of Σ and K^* exchanges in this reaction. In contrast, K and proton exchanges play a more significant role in this reaction, making the uncertainty associated with $g_{NK\Lambda}$ potentially influential on the final results. However, our detailed calculations show that such changes can be effectively compensated by adjusting the fitted cutoff parameter Λ_M within a reasonable range of 1.1–1.4 GeV during the fitting process. Furthermore, we observe that the fitted parameters for resonances remain largely unaffected by these changes. To further illustrate the effects of varying $g_{\Lambda NK}$ on our fitting results, Fig. 6 presents the results obtained using different values of $g_{\Lambda NK}$ at $p_K = 514$ MeV and 714 MeV. These plots demonstrate how changes in $g_{\Lambda NK}$ influence the quality of our fits.

Regarding the results presented above, it seems that due to the relatively large uncertainties of the experimental data, we cannot distinguish various models well. To verify these models, it is helpful to study their predictions for spin observables. In Fig. 7, we present the predictions of the spin polarization of Λ perpendicular to the scattering plane using the various models. It is found that the models give distinct predictions for this observable, which are mainly caused by the different interference patterns of the background and various resonance contributions. These results show that future measurements of P_Λ should be helpful for verifying these models.

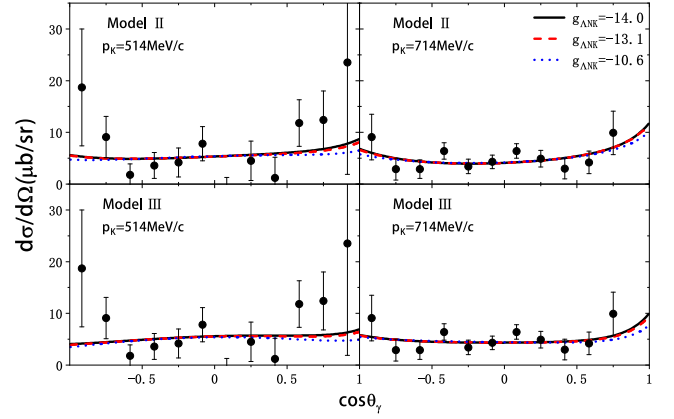


Fig. 6. (color online) Fitting results with different values of the coupling constant $g_{\Lambda NK}$ [10, 27].

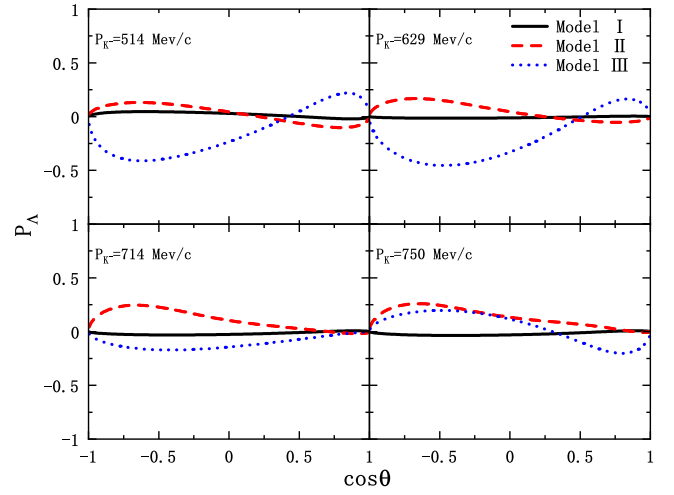


Fig. 7. (color online) Polarization of Λ perpendicular to the scattering plane considering the background and various resonance contributions.

V. SUMMARY

In this work, we studied the $K^-p \rightarrow \gamma\Lambda$ reaction using an effective Lagrangian approach and isobar model while explicitly considering the t -channel (K and K^*) and u -channel (proton) exchanges as the background contribution. We found that the background contribution plays an important role in this reaction. It was also found that $\Lambda(1520)$ may contribute significantly at the near-threshold region, and $\Sigma(1650)$ or $\Sigma(1670)$ may contribute to this reaction at higher energies. Meanwhile, due to the uncertainties of the experimental data, we cannot distinguish various models well. Our work shows that more accurate data, especially at backward angles, are essential for studying the background contribution and the two GIR methods adopted in this work. Furthermore, the polarization of Λ is sensitive to the reaction mechanism and suitable for verifying the background contribution and

References

- [1] A. Thiel, F. Afzal, and Y. Wunderlich, *Prog. Part. Nucl. Phys.* **125**, 103949 (2022), arXiv: 2202.05055
- [2] F. X. Lee, T. Mart, C. Bennhold *et al.*, *Nucl. Phys. A* **695**, 237 (2001), arXiv: nucl-th/9907119
- [3] S. Janssen, J. Ryckebusch, D. Debruyne *et al.*, *Phys. Rev. C* **65**, 015201 (2002), arXiv: nucl-th/0107028
- [4] S. Janssen, J. Ryckebusch, W. Van Nespen *et al.*, *Eur. Phys. J. A* **11**, 105 (2001), arXiv: nucl-th/0105008
- [5] S. Janssen, D. G. Ireland, and J. Ryckebusch, *Phys. Lett. B* **562**, 51 (2003), arXiv: nucl-th/0302047
- [6] D. Petrellis and D. Skoupil, *Phys. Rev. C* **107**, 045206 (2023), arXiv: 2212.14305
- [7] N. H. Luthfiyah and T. Mart, *Phys. Rev. D* **104**, 076022 (2021), arXiv: 2110.01789
- [8] A. Fatima, Z. Ahmad Dar, M. Sajjad Athar *et al.*, *Int. J. Mod. Phys. E* **29**, 2050051 (2020), arXiv: 2001.10201
- [9] T. Mart, *Phys. Rev. D* **100**, 056008 (2019), arXiv: 1909.02696
- [10] D. Skoupil and P. Bydžovský, *Phys. Rev. C* **93**, 025204 (2016), arXiv: 1601.03840
- [11] D. Skoupil and P. Bydžovský, *Phys. Rev. C* **97**, 025202 (2018), arXiv: 1801.07466
- [12] T. Mart and C. Bennhold, *Phys. Rev. C* **61**, 012201 (2000), arXiv: nucl-th/9906096
- [13] S. Clymton and T. Mart, *Phys. Rev. D* **96**, 054004 (2017)
- [14] B. Julia-Diaz, B. Saghai, F. Tabakin *et al.*, *Nucl. Phys. A* **755**, 463 (2005)
- [15] V. Shklyar, H. Lenske, and U. Mosel, *Phys. Rev. C* **72**, 015210 (2005)
- [16] R. Shyam, O. Scholten, and H. Lenske, *Phys. Rev. C* **81**, 015204 (2010)
- [17] B. Julia-Diaz, B. Saghai, T.-S. Lee *et al.*, *Phys. Rev. C* **73**, 055204 (2006)
- [18] T. Corthals, J. Ryckebusch, and T. Van Cauteren, *Phys. Rev. C* **73**, 045207 (2006), arXiv: nucl-th/0510056
- [19] P. Vancraeyveld, L. De Cruz, J. Ryckebusch, and T. Van Cauteren, *Phys. Lett. B* **681**, 428 (2009), arXiv: 0908.0446
- [20] R. Williams, C. R. Ji, and S. R. Cotanch, *Phys. Rev. D* **41**, 1449 (1990)
- [21] S. Prakhov *et al.*, *Phys. Rev. C* **82**, 015201 (2010), arXiv: 0912.1653
- [22] T. Van Cauteren, J. Ryckebusch, B. Metsch *et al.*, *Eur. Phys. J. A* **26**, 339 (2005), arXiv: nucl-th/0509047
- [23] T. Van Cauteren, J. Ryckebusch, B. Metsch *et al.*, *Eur. Phys. J. A* **31**, 613 (2007)
- [24] S. Navas *et al.* (Particle Data Group), *Phys. Rev. D* **110**, 030001 (2024)
- [25] A.-C. Wang, W.-L. Wang, and F. Huang, *Phys. Rev. D* **101**, 074025 (2020), arXiv: 2002.04213
- [26] N.-C. Wei, A.-C. Wang, F. Huang *et al.*, *Phys. Rev. D* **105**, 094017 (2022)
- [27] J. J. de Swart, *Rev. Mod. Phys.* **35**, 916 (1965), [Erratum: *Phys. Rev. C* **37**, 326 (1965)]
- [28] J.-J. Xie, E. Wang, and J. Nieves, *Phys. Rev. C* **89**, 015203 (2014)
- [29] A. Wang, W. Wang, F. Huang *et al.*, *Phys. Rev. C* **96**, 035206 (2017)
- [30] S.-H. Kim, S.-i. Nam, Y. Oh *et al.*, *Phys. Rev. D* **84**, 114023 (2011)
- [31] K. Ohta, *Phys. Rev. C* **40**, 1335 (1989)
- [32] R. Davidson and R. Workman, *Phys. Rev. C* **63**, 025210 (2001)
- [33] H. Haberzettl, *Phys. Rev. C* **56**, 2041 (1997)
- [34] H. Haberzettl, C. Bennhold, T. Mart *et al.*, *Phys. Rev. C* **58**, R40 (1998)
- [35] F. Huang, M. Döring, H. Haberzettl *et al.*, *Phys. Rev. C* **85**, 054003 (2012)
- [36] J. C. Ward, *Phys. Rev.* **78**, 182 (1950)
- [37] Y. Takahashi, *Nuovo Cim.* **6**, 371 (1957)
- [38] Y. Oh, C. M. Ko, and K. Nakayama, *Phys. Rev. C* **77**, 045204 (2008)
- [39] J. Shi and B.-S. Zou, *Phys. Rev. C* **91**, 035202 (2015), arXiv: 1411.0486